ISSN 2063-5346

THERAPEUTIC POTENTIAL OF SILVER NANOPARTICLES IN HEALING OF CORNEAL ULCER INDUCED IN DIABETIC ALBINO RAT MODEL: A HISTOLOGICAL, IMMUNOHISTOCHEMICAL AND BIOCHEMICAL STUDY

Fayza Abdel Raouf Abdel Gawad [1], Walaa Mohamed Sayed[1], Marwa Mohamed Abdel Gawad[2], Asmaa Sayed Mohamed[1], Abdel Satar Abdel Satar Ibrahim[1]

Article History: Received: 02.07.2023 Revised: 15.07.2023 Accepted: 23.07.2023

Abstract

Background: Diabetic keratopathy is a potentially sight-threatening condition caused by epithelial and stromal disturbances, it exhibits several clinical manifestations, including persistent corneal epithelial erosions and resistant ulcers.

Aim of work: to demonstrate the histological and biochemical changes in diabetic keratopathy, and to assess the effect of AgNps in healing of corneal ulcer in diabetic rat model.

Material & Methods: In the current study, 55 adult male albino rats were allocated into 4 groups; group I, normal control, group II, diabetic keratopathy group, that received alloxan drug for induction of diabetes, group III, corneal ulcer group, that underwent corneal ulcer induction by NaOH solution under general anesthesia, group IV, AgNps-treated group. Cornea were extracted from each group on three time points; day 0, day 2 and day 7, and were subjected to histological, immunohistochemical and biochemical assay.

Results: Diabetic keratopathy corneae showed apoptotic cellular and stromal changes, in addition to over expression of matrix metalloproteinases and growth factors. While, corneal ulcer group elicited epithelial loss, surge of the corneal tissue levels of metalloproteinases. AgNps-treated corneae showed histological improvement in corneal sections, improved apoptotic and inflammatory markers, in addition to upregulation of PI3K/AKT/MTOR signaling pathway.

Conclusion: AgNps were found to be promising in improving healing of corneal ulcer in resistant conditions such as DM.

Key words: Diabetic keratopathy, TGF, MMPs, NGF, TrKA, Oxidative stress.

[1] Department of Anatomy and Embryology, Faculty of Medicine, Cairo University.
[2] Department of Clinical Biochemistry, Faculty of Medicine, Cairo University.

DOI:10.48047/ecb/2023.12.9.232

Introduction

Diabetic keratopathy (DK) is a potentially sight-threatening condition caused mostly by epithelial disturbancesm it exhibits several clinical manifestations, including persistent corneal epithelial erosion, superficial punctate lesions, delayed epithelial regeneration and resistant corneal ulcers. (***Priyadarsini et al., 2020).*** Delayed healing of corneal wounds in diabetes mellitus (DM) is a challenging clinical problem, as elevated blood glucose level hinders proliferation of cells and decreases neocollagenesis. DM is associated with decreased chemotaxis and fibroblast proliferation, that contribute to the observed impairment in epithelial rejuvenation in diabetic patients ***(Rezvanian et al., 2021).*** Regulation of corneal epithelial healing is a cascade of signals orchestrated by numerous growth factors and cytokines, mainly transforming growth factor beta (TGF β), platelet-derived growth factor (PDGF), nerve growth factor (NGF), interleukin 6 (IL-6) and interleukin 10 (IL-10). These various factors lead to imbalance between cellular migration, proliferation, differentiation and apoptosis ***(Yeung et al., 2021).*** Hyperglycemia triggers the expression of various cytokines and cell adhesion molecules. Over-expression of chemokines, pro-inflammatory proteins and pro-apoptotic genes is a key contributor to developing diabetic keratopathy (***Kramerov et al., 2021).*** Keratocyte activation and tissue fibrosis all participate in the ulcer healing process. Under normal conditions, corneal keratocytes are constant in number and help maintain corneal transparency. However, after corneal injury, disruption of corneal integrity, stimulates many cytokines and growth factors that affect the corneal wound healing process. Metal nanoparticles (e.g., silver and zinc) are increasingly being used in medicine, besides their beneficial effect on epithelial rejuvenation and bacterial infections prevention, they are affordable and easy to use ***(Mihai et al., 2019).*** It has been suggested that silver nanoparticles (AgNPs) can support corneal ulcer healing through both inhibition of bacterial growth the production of pro-inflammatory cytokines such as IL-6 and TGF, it also exhibits a broad-spectrum antibacterial capability against many micro-organisms, and thus represent a potential alternative to overcome the emerging issues of microbial resistance (***Kalantari et al., 2020).*** Silver can ameliorate the oxidative stress status in DM ***(Afifi and Abdel Azim, 2015),*** it is postulated to increase the genetic expression of antioxidant enzymes levels (***Torabian et al., 2022).*** It possess unique electronic and optical properties due to their negative charges, which in turn prevent aggregation of the particles. They offers an optimal opportunity to conjugate ligands such as thiols therefore they are a better antioxidant than the silver salt itself (***Mauricio et al., 2013).***

Aim of work: The current work aimed to assess the effect of AgNps on healing of induced corneal ulcer in diabetic rats, in addition to demonstrating the histological and biochemical changes of diabetic keratopathy.

Material and Methods

Induction of DM: Alloxan monohydrate 98% (powder) was purchased from Sigma Aldrich Co., Cairo, Egypt. After dilution in sesame oil (0.1 g alloxan monohydrate/0.9 ml sesame oil), rats were injected intravenously through the tail vein with a single dose of alloxan (40 mg/kg BW). After 48 hours of alloxan administration, blood samples were collected from tail veins for measuring blood glucose levels to ensure the establishment of DM; only rats with blood glucose level ≥ 250 mg/dl in two successive measurements were employed in the experiment ***(Majeed et al., 2018)***.

Induction of corneal ulcer: Animals allocated for corneal ulcer received anesthesia using a combination of intramuscular injection of ketamine 50 mg/kg (Pfizer Inc., Germany) and midazolam 1 mg/kg (Dormicum; Pfizer Inc., Germany). Right corneae only

received induction of ulcer, while the left corneae were left to allow free vision and movements of rats. Sterilization of surgical surface was done by 10% polyvinylpyrrolidone iodine solution. After application of an eye retractor, a 3.5 mm thickness filter paper disc soaked in 1N sodium hydroxide was applied to the center of the right cornea of each rat for 30 sec (***Kim et al., 2021)***. Corneae were washed thoroughly after removing the paper disc with 10 ml of phosphate buffered saline (PBS). Day of induction of corneal ulcer was considered day zero of the experiment.

Experimental animals: The study was conducted on 55 adult male albino rats, weighing 150 - 200 g, provided by the Animal House, Kasr AlAiny, Faculty of Medicine, Cairo University. The rats were housed according to the ethical guidelines for the Care and Use of Laboratory animals. They were housed in special metal cages, each 40x30x16 cm and exposed to a light/dark cycle at 14:10-hour photo cycle at 22-24°C under standard laboratory and environmental conditions. The animals were provided with standard rodent food pellets and water *ad libitum.* Rats were acclimatized for two weeks before proceeding into the experiment. The approval of the Institutional Animal Care and Use Committee, Cairo University (IACUC-CU) was obtained before proceeding into the experiment and the approval number is CU/III/F/60/21.

Study design: Rats were allocated into 4 groups; Group I (normal control): 15 rats, that received no manipulation; 5 rats were sacrificed on day zero, 5 rats were sacrificed on day 2 and 5 rats were sacrificed on day 7 of the experiment. Group II (diabetic keratopathy): 15 rats were subjected to induction of DM with no surgical procedures; 5 rats were sacrificed on day zero, 5 rats were sacrificed on day 2 and 5 rats were sacrificed on day 7 of the study. Group III (corneal ulcer): 15 diabetic rats were subjected to induction of corneal ulcer in the right eyes; 5 rats were sacrificed on day zero, 5 rats were sacrificed on day 2 and 5 rats were sacrificed on day 7 of the experiment ***(Kim et al., 2021)***. Group V (AgNps-treated): 10 diabetic rats, that received daily subconjunctival injection of AgNps in the right eyes (0.1 mg/ml), started after induction of corneal ulcer ***(Butler et al., 2015)***, silver nanoparticles (10 ppm) was purchased from Nanotech Company for Photoelectronics, Cairo, Egypt, in the form of liquid suspension. 5 rats were sacrificed on day 2 and 5 rats were sacrificed on day 7 of the experiment. The animals were sacrificed by cervical dislocation, after light ether inhalation, to avoid chemical injury. After sacrification, the animals' corneae were removed 1 mm close to limbus. Parts of the collected corneae were fixed in 10% formaldehyde solution for histological and immunohistochemical studies, to be examined by light microscopy, and other parts were preserved in PBS for biochemical study.

Histological and immunohistochemical study: Corneal sections were deparafinized in xylene and washed in descending grades of ethanol (100%, 95%, and 70%) 5 minutes each, then rehydrated in phosphate buffer saline (PBS) by using a steamer in citrate buffer with pH 6.0 for 15 min and endogenous peroxidase activity was blocked with H2O2 in methanol. Sections were incubated at room temperature with rabbit monoclonal MMP-2, TrKA and TGF-beta. Ultra Vision detection System (Thermo Scientific) was used as follows: sections were incubated with biotinylated goat anti-polyvalent, then with streptavidin peroxidase and finally with DAB plus chromogen. Slides were counterstained with haematoxylin dehydrated in alcohol and xylene and covered with neutral balsam. The slides were visualized under light microscope and the extent of cell immune positivity was assessed in all groups by Image J analyser computer software program in MMP-2, TrKA and TGF-β stained sections, they were examined within the standard measuring frame of a known area equal to

11694.91µm^2, and data were expressed as mean values.

Biochemical study: Parts of the cornea obtained from each animal were prepared with 0.1 ml of PBS solution and centrifuged at 1200 rpm for 10 min ***(Wang et al., 2019)*.** The supernatant was used to measure the tissue levels of: 1- MMP-9, it was detected using Mouse MMP-9 ELISA Kit (Catalog M1000, R&D Systems, Minneapolis, M. N.), according to the manufacturer's instructions. Detection limit was 1 pg/ml. 2- Anti P75, it was detected using Rat Anti-P75 Platinum ELISA kit (eBioscience, Inc.) following the manufacturer's protocols. Detection limit was 1pg/ml. 3- IL-6 It was detected using Mouse IL-6 ELISA Kit (Catalog M1000, R&D Systems, Minneapolis, M. N.), according to the manufacturer's instructions. Detection limit was 4pg/ml. 4- PDGF, it was detected using Mouse PDGF ELISA Kit (Catalog M1000, R&D Systems, Minneapolis, M. N.), according to the manufacturer's instructions. Detection limit was 1pg/ml. 5- ROS and MDA were detected by colormetry. 6- Genetic expression of PI3K, AKT and MTOR genes were evaluated using PCR, total RNA extraction was done from phosphate buffer preserved corneal tissue homogenate using the TRIzol method according to the manufacturer's protocol. The cDNA was synthesized from 1 ug RNA using Superscript III First-Strand Synthesis; a system described in the manufacturer's protocol (Invitrogen, Life Technologies). The relative abundance of mRNA species was assessed using the SYBR Green method on an ABI prism 7500 sequence detector system (Applied Biosystems, Foster City, CA). PCR primers were designed with Gene Runner Software (Hasting Software, Inc., Hasting, NY) from RNA sequences from Gen Bank **(Table 1).** Data from real-time assays were calculated using the v1·7 Sequence Detection Software from PE Biosystems (Foster City, CA). Relative expression of studied gene mRNA was calculated using the comparative Ct method. All values were normalized to the beta actin gene and reported as fold change.

Statistical analysis: The obtained data were recorded using Microsoft Excel worksheet, 2020. Statistical analysis was performed using Statistical Package for the Social Sciences (SPSS) version 21.0 (IBM Corporation, Somers, NY, USA) statistical software. The data were expressed as means ± standard deviation (SD). Statistical evaluation was done using one-way analysis of variance (ANOVA). Significance was considered when p value was equal to or less than 0.05 throughout the study.

Table 1 : Primer sequences of AKT, PI3K, MTOR genes and beta actin

Gene	Primer sequence 5' – 3	Fragment size
AKT	Fw: TTCTGCAGCTATGCGCAATGTG Rv: GAACTGCAGTGCACCTTTCAAGC	108
PI3K	Fw: GGTTGTCTGTCAATCGGTGACTGT Rv: TGGCCAGCATACCATAGTGAGGTT	181
MTOR	Fw: GCTTGATTTGGTTCCCAGGACAGT Rv: GTGCTGAGTTTGCTGTACCCATGT	194
β actin	Fw: TCCCTGGAGAAGAGCTACG Rv: GTAGTTTCGTGGATGCCACA	131

AKT : serine/threonine-protein kinase, PI3K: phosphatidylinositol-3-kinase, MTOR: mammalian target of rapamycin.

Results

Histological results

Hx & E- stained sections

Corneal sections of the control group in rats sacrificed on day 0, 2 and 7 showed 3 distinct zones, outer epithelium, intermediate stroma, and inner endothelium. The corneal epithelium appeared as a non-keratinized stratified squamous epithelium arranged in 3 layers. The basal layer formed of columnar cells, the intermediate layer consisted of polygonal cells and the superficial layer formed of flat squamous cells. The epithelium was resting on an underlying well distinct Bowman's membrane**.** The corneal stroma showed regular parallel lamellae of collagen fibrils with few keratocytes in between them. The endothelium is made up of a single cell layer supported by intact Descemet's membrane **(Fig 1A)**. On day zero, DK group showed nearly normal corneal structure **(Fig. 1B).** On day two, DK group cornea elaborated vacuolated cytoplasm in some epithelial cells, and areas of widely spaced collagen fibers in the stroma (**Fig. 1C**). On day seven, corneal sections showed structural and cellular changes; some corneal epithelial cells revealed pyknotic nuclei, while some cells showed vacuolated cytoplasm with eccentric nuclei. The stroma exhibited areas of widely spaced collagen fibers, sub-epithelial vascularization and inflammatory cell infiltration. The Descemet's membrane appeared relatively thick and wavy (**Fig. 1D)**. Regarding corneal ulcer group, corneal sections harvested on day zero showed marked corneal epithelial discontinuity; complete separation of the epithelium from the underlying stroma, with disrupted Bowmam's membrane, inflammatory cellular infiltration and invasion with small blood vessels were observed in between the irregularly dispersed collagen fibers of the stroma **(Fig. 1E).** Most corneal sections obtained from rats sacrificed on day 2 showed focal areas of epithelial discontinuity. The stromal collagen fibers were disorganized with wide spacing, extensive vascularization as well as cellular infiltration **(Fig. 1F).** Most sections obtained from rats sacrificed on day 7 showed disrupted epithelium with epithelial discontinuity in some areas, in addition to disrupted Bowman's membrane. Some corneal sections showed multiple cells with vacuolated cytoplasm and karyolytic nuclei, other epithelial cells appeared pyknotic. The stroma exhibited inflammatory cellular infiltrates and extensive vascularization **(Fig. 1G)**. In AgNps-treated group, on day two of the experiment, corneal sections elicited epithelial discontinuity, with areas of complete epithelial loss. Several sections showed disorganized stromal fibers; widely dispersed collagen fibrils as well as extensive corneal vascularization **(Fig. 1H).** While rats sacrificed on day 7 showed epithelial regeneration in most parts of the stained corneae, re-arrangement of stromal collagen fibers with cellular infiltrates, intact Descemet`s membrane and endothelium were denoted **(Fig. 1I).** Mean corneal thickness was significantly decreased in DK group (days 2 and 7), compared with control group cornea collected on the same days, it was significantly decreased as well in corneal ulcer group collected on days 0,2 and 7, in comparison with control and DK corneae collected on the same days. AgNps-treated group elicited a significant increase in the mean corneal thickness in corneae collected on days 2 and 7 compared to DK and corneal ulcer groups **(Fig. 2).**

PAS- stained sections

Corneal sections of the control group **(Fig. 3A**) as well as DK group harvested on days zero **(Fig. 3B**) and two (**Fig. 3C**) showed positive PAS reaction in the superficial epithelial layer, Bowman's membrane and Descemet's membrane. In DK group

sections collected on day seven (**Fig. 3D**) showed negative PAS reaction. Corneal ulcer group cornea collected on day 0 and 2 (**Fig. 3E, 3F)** showed negative PAS reaction, while cornea collected on day 7 (**Fig 3G)** elicited positive PAS reaction in superficial epithelial layer and Descemet's membrane. AgNps treated group exhibited positive PAS reaction in corneae collected on days 2 and 7 **(Fig. 3H, 3I).** Descemet's membrane thickness was significantly increased in DK group corneae on days 2 and 7, compared with control group, while corneal ulcer group showed a significant decreament in Descemet's membrane thickness on days 0, 2 and 7. AgNps treated group elicited a significant rise in Descemet's membrane thickness on days 2 and 7, in comparison with corneal ulcer group **(Fig. 4).**

Immunohistochemical results

MMP-2 stained sections

MMP-2 reaction was negative in control group corneae and DK corneae harvested on day 0, while corneae collected on days 2 and 7 elicited positive MMP-2 immune reaction in basal epithelial cells, stromal cells and some endothelial cells as well. In corneal ulcer group, positive reactivity was detected on days zero, two and seven in most corneal epithelial cells. AgNps treated group showed positive MMP-2 reaction in most epithelial cells on day 2 and in few basal cells on day 7 **(Fig. 5**). Mean area % of immunoreactivity was significantly higher in DK group corneae harvested on days 2 and 7, compared with control group specimens collected on the same days. Corneal ulcer group also showed a significantly higher mean area of reactivity on days 0, 2 and 7, compared with control group and DK group collected on the same days. AgNps-treated corneae elicited a decreased mean area % of reaction on days 2 and 7 **(Fig. 6).**

TrKA- stained sections

Control group cornea and DK cornea collected on day 0 elicited no reaction to TrKA antigen, while corneae collected on days 2 and 7 elicited positive TrKA membranous immune reaction in epithelial cells. In corneal ulcer group, positive membranous and cytoplasmic reactivity was detected on days zero, two and seven in most epithelial cells. AgNps-treated group showed positive MMP-2 reaction in some epithelial cells on day 2 and 7 **(Fig. 7).** Mean area % of immunoreactivity was significantly higher in DK group corneae harvested on days 2 and 7, compared with control group specimens collected on the same days. Corneal ulcer group also showed a significantly higher mean area of reactivity on days 0, 2 and 7, compared with control group and DK group collected on the same days. AgNps-treated corneae elicited a decreased mean area % of reaction on days 2 and 7 (**Fig. 8).**

TGF- beta stained sections

Regarding TGF-β, immune reaction was negative in control group corneae as well as DK corneae harvested on day 0, corneae collected on days 2 and 7 elicited positive cytoplasmic reaction in epithelial cells and stromal cells as well. In corneal ulcer group, positive reactivity was detected on days zero, two and seven in most corneal epithelial cells. AgNps treated group showed positive cytoplasmic TGF- β reaction in some epithelial cells on days 2 and 7 (**Fig. 9).** Mean area % of immunoreactivity was significantly higher in DK group corneae harvested on days 2 and 7, compared with control group specimens collected on the same days. Corneal ulcer group also showed a significantly higher mean area of reactivity on days 0, 2 and 7, compared with control group and DK group collected on the same days. AgNps-treated group showed a significant decline in the mean area % of reaction on days 2 and 7, compared to DK and corneal ulcer groups (**Fig. 10).**

Biochemical results (Table 2)

Mean tissue level of MMP-9 was elevated in DK and corneal ulcer groups, in comparison with normal control group, AgNps treated group showed a significant decline in its tissue levels on days 2 and 7, compared to DK and corneal ulcer groups

harvested on the same days (histogram 6). Anti P75 was elevated as well in DK (day 2 and 7) and corneal ulcer (day 0, 2 and 7) groups, compared with control group, however, AgNps-treated corneae elicited a significant decline in its tissue levels, on days 2 and 7 (histogram 7). As for PDGF and IL-6 they both showed a significant rise in DK and diabetic ulcer group corneae on days 0, 2 and 7, in comparison with control group. AgNps-treated group elicited a significant decrease in its mean tissue level on days 2 and 7, in comparison with DK and diabetic ulcer group (histograms 8, 9). ROS tissue levels was significantly increased in DK and diabetic ulcer group, versus control group, however, AgNps treated group showed a significant decrease in its tissue levels on days 2 and 7 (histogram 10). Regarding MDA tissue levels, it was significantly increased in DK and diabetic ulcer groups, AgNps treated group showed insignificant change in MDA tissue levels, compared to DK and diabetic ulcer groups.

Gene expression of AKT/PI3K/MTOR pathway

Real time PCR elaborated inhibited PI3K/AKT/MTOR pathway in the DK group cornea, harvested on days two and seven, compared to control group cornea harvested on the same days. However, in corneal ulcer group, PI3K/AKT/MTOR axis was up-regulated in cornea collected on days zero, two and seven, in comparison to DK and control groups. In AgNps-treated rats, PI3K/AKT/MTOR pathway was activated and expression of the three genes was increased; in cornea collected on days two and seven, in comparison to corneal ulcer and DK groups **(Fig. 11).**

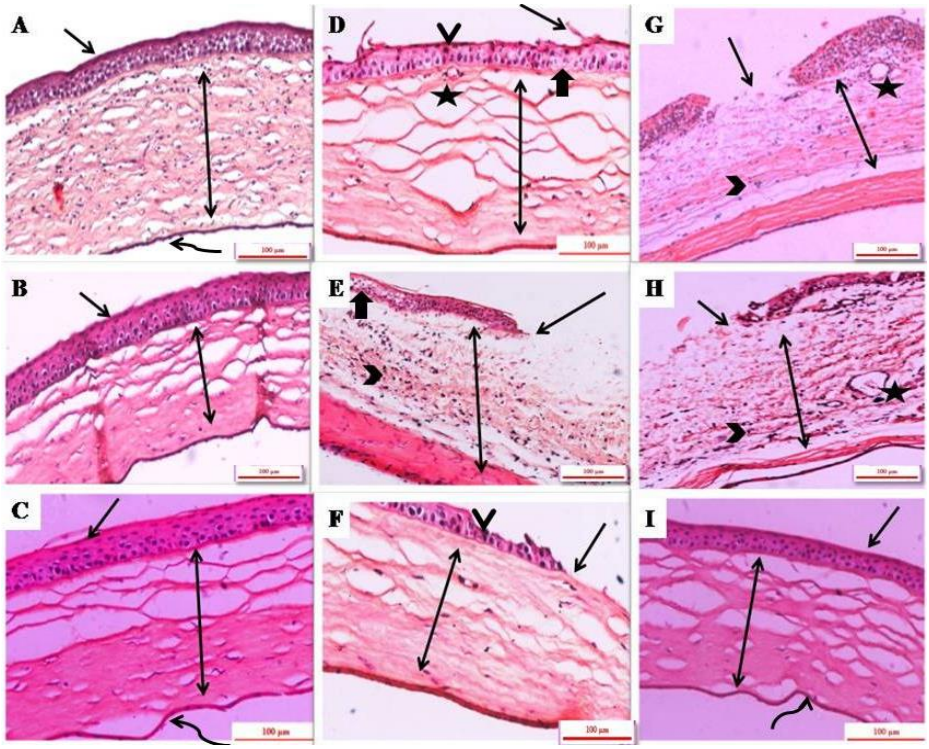

Fig. 1: Photomicrographs of Hx&E stained sections of the different study groups, A: normal control group, B: DK group day 0, C: DK group day 2, D: DK group day 7, E: diabetic ulcer group day 0, F: diabetic ulcer group day 2, G: diabetic ulcer group day 7, H: AgNps-treated group day 2, I: AgNps treated group day 7, arrow: corneal epithelium, double arrow: stromal collagen, curved arrow: Descemets membrane, *: blood vessel, chevron: inflammatory cells, thick arrow: vacuolated cells, arrow heads: pyknotic nuclei.

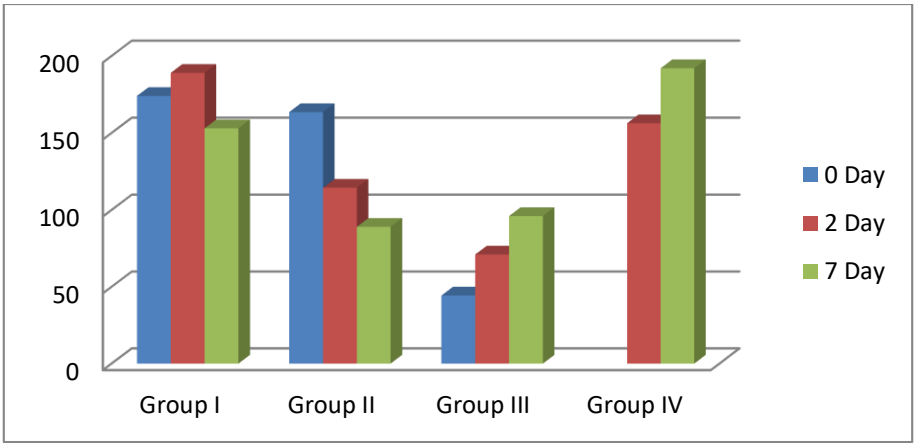

Fig. 2: A histogram showing mean corneal thickness among different groups

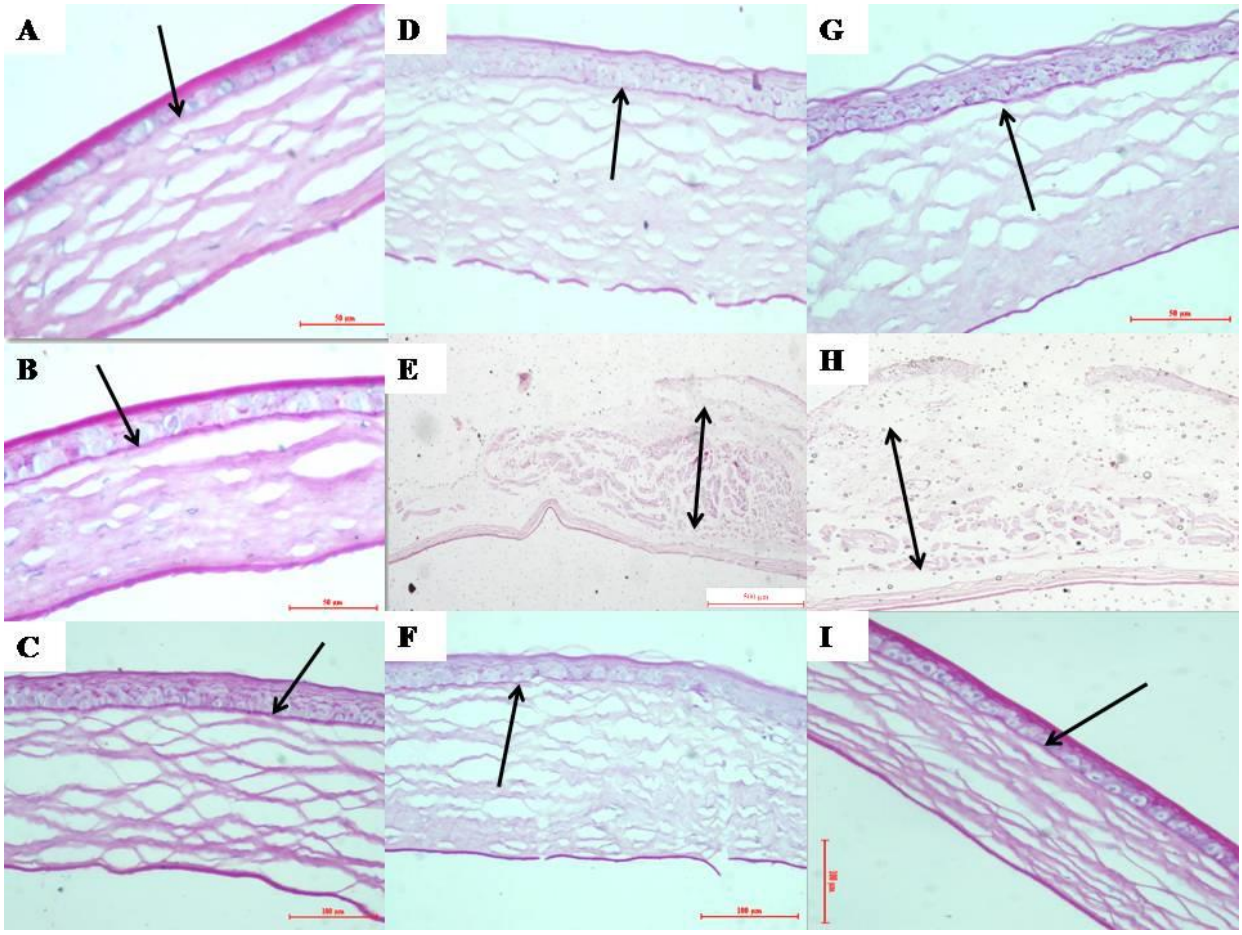

Fig. 3: Photomicrographs of PAS stained sections of the different study groups, A: normal control group, B: DK group day 0, C: DK group day 2, D: DK group day 7, E: diabetic ulcer group day 0, F: diabetic ulcer group day 2, G: diabetic ulcer group day 7, H: AgNps-treated group day 2, I: AgNps-treated group day 7, arrow: Bowman's membrane, double arrow: fragmented collagen fibrils.

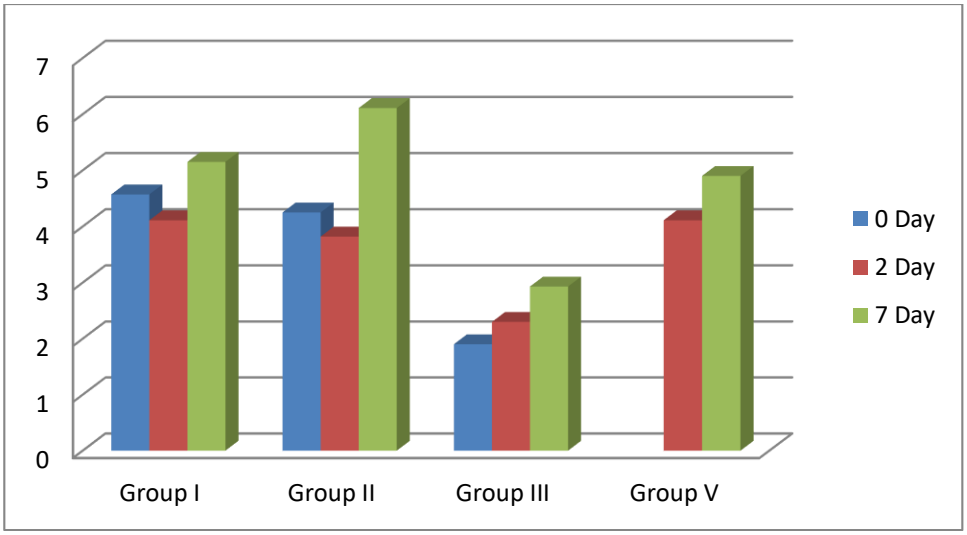

Fig. 4: A Histogram showing Descemet's membrane thickness in different groups.

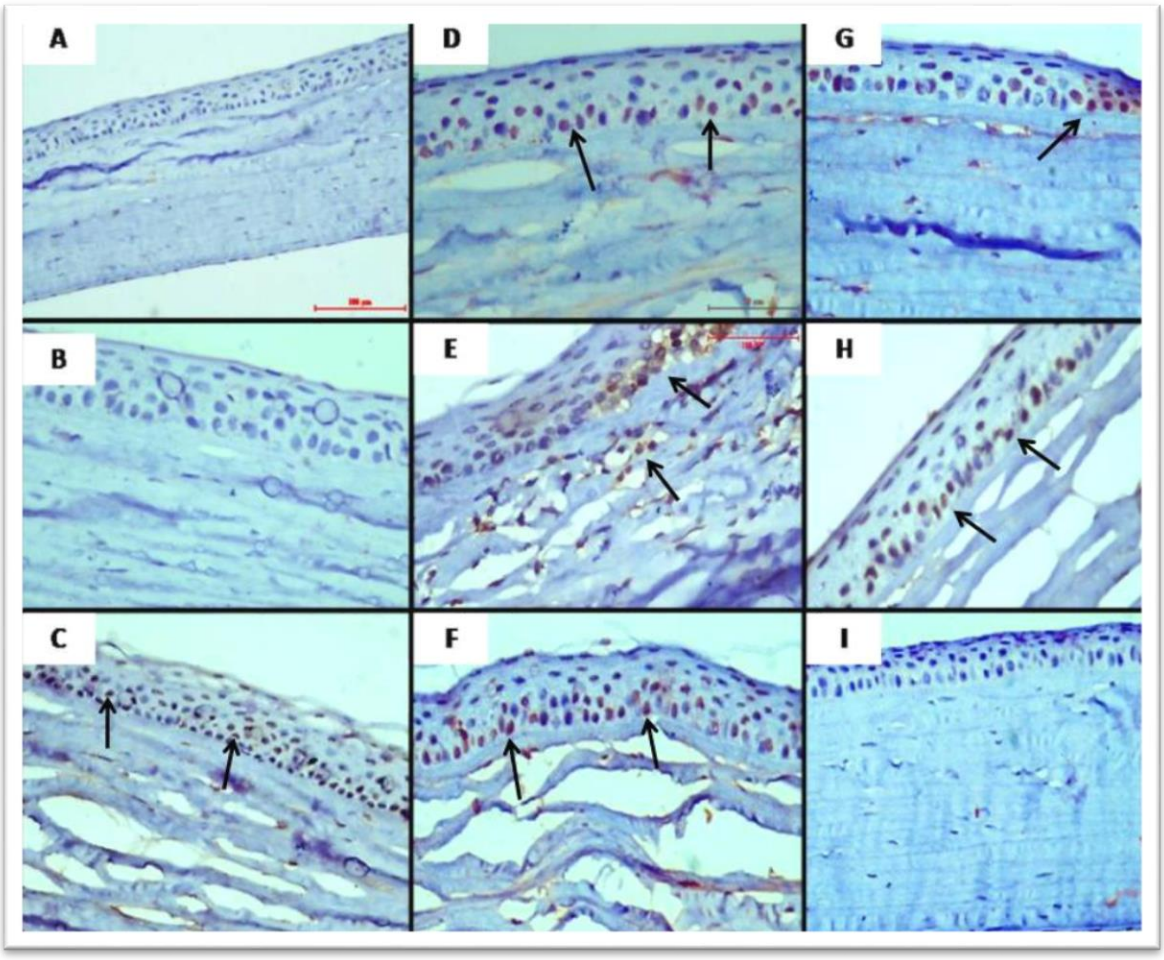

Fig. 5: Photomicrographs of MMP-2 stained sections of the different study groups, A: normal control group, B: DK group day 0, C: diabetic ulcer group day 0, D: DK group day 2, E: diabetic ulcer group day 2, F: AgNps treated group day 2, G: DK group day 7, H: diabetic ulcer group day 7, I: AgNps treated group day 7, arrows: immunopositive cells.

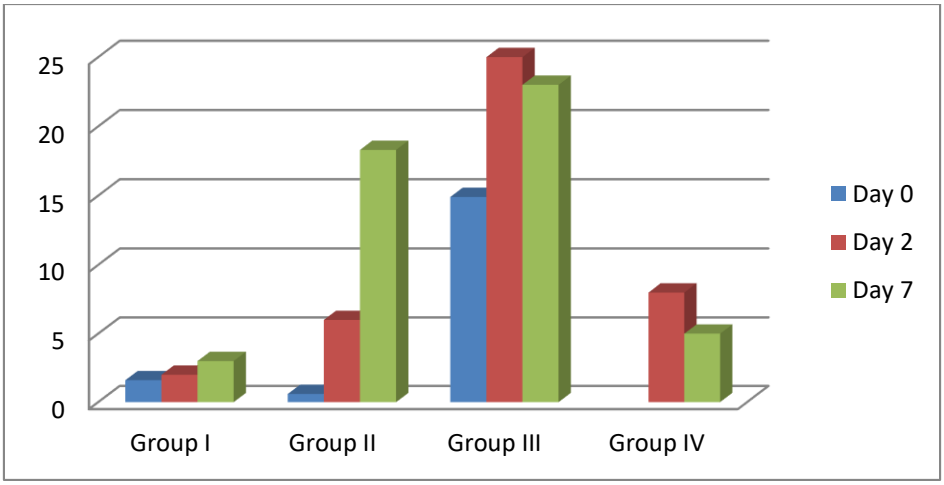

Fig. 6: A histogram showing MMP-2 immunoreactivity in different groups

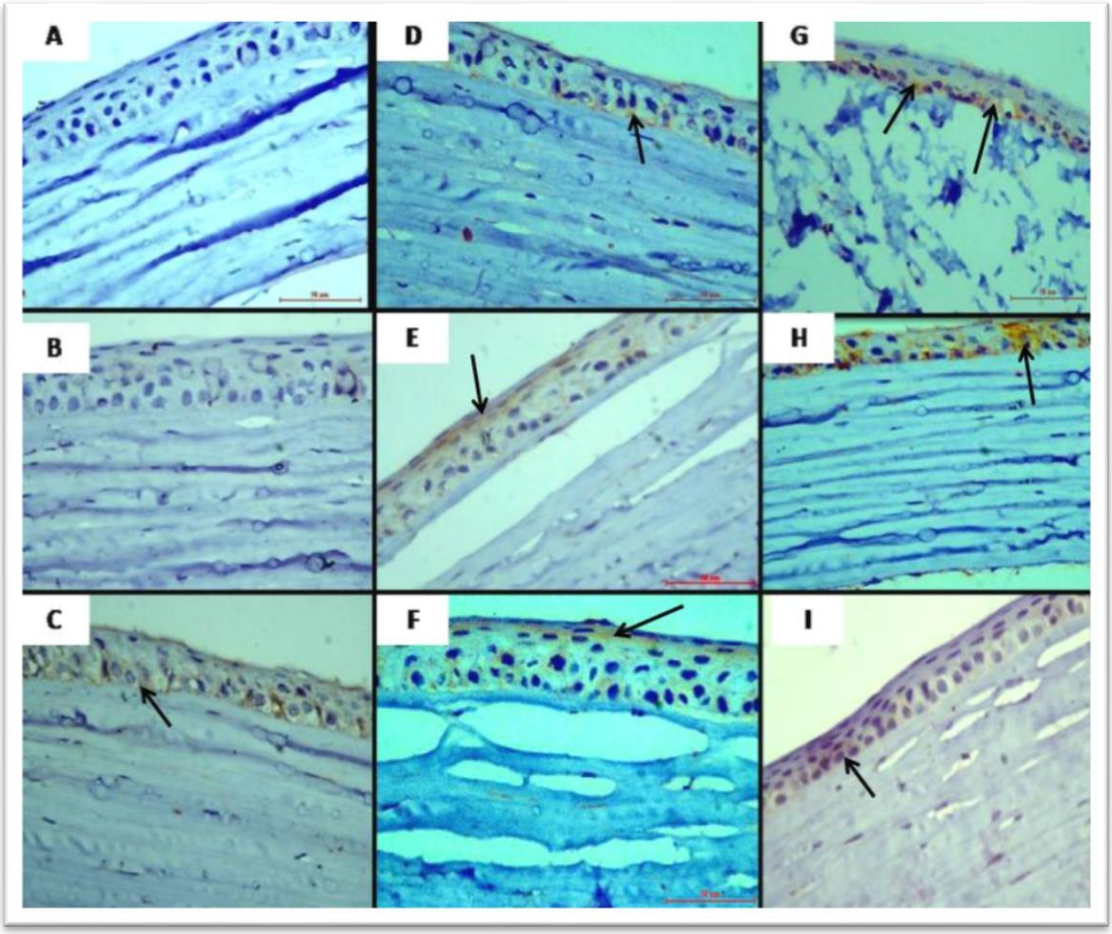

Fig. 7: Photomicrographs of TrKA stained sections of the different study groups, A: normal control group, B: DK group day 0, C: diabetic ulcer group day 0, D: DK group day 2, E: diabetic ulcer group day 2, F: AgNps treated group day 2, G: DK group day 7, H: diabetic ulcer group day 7, I: AgNps treated group day 7, arrows: immunopositive cells.

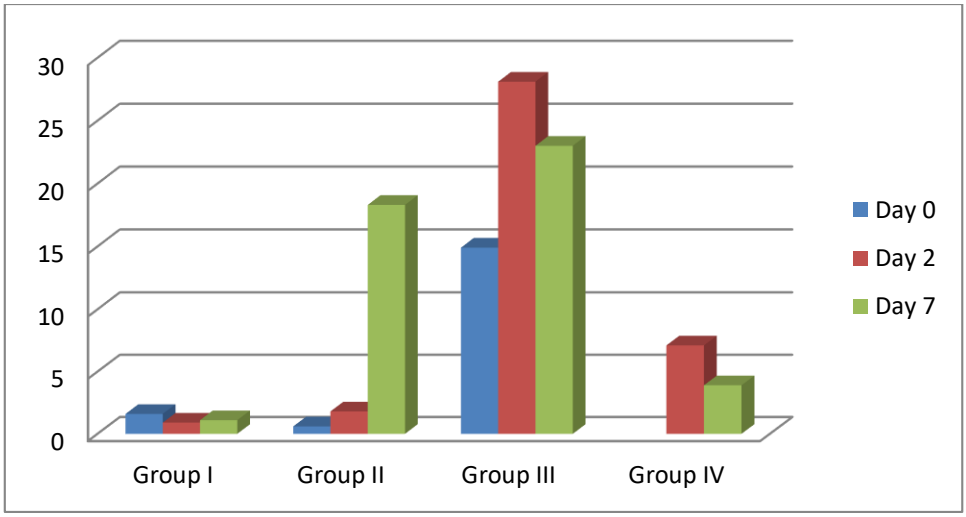

Fig. 8 : A histogram showing TrKAimmunereactivity in different groups

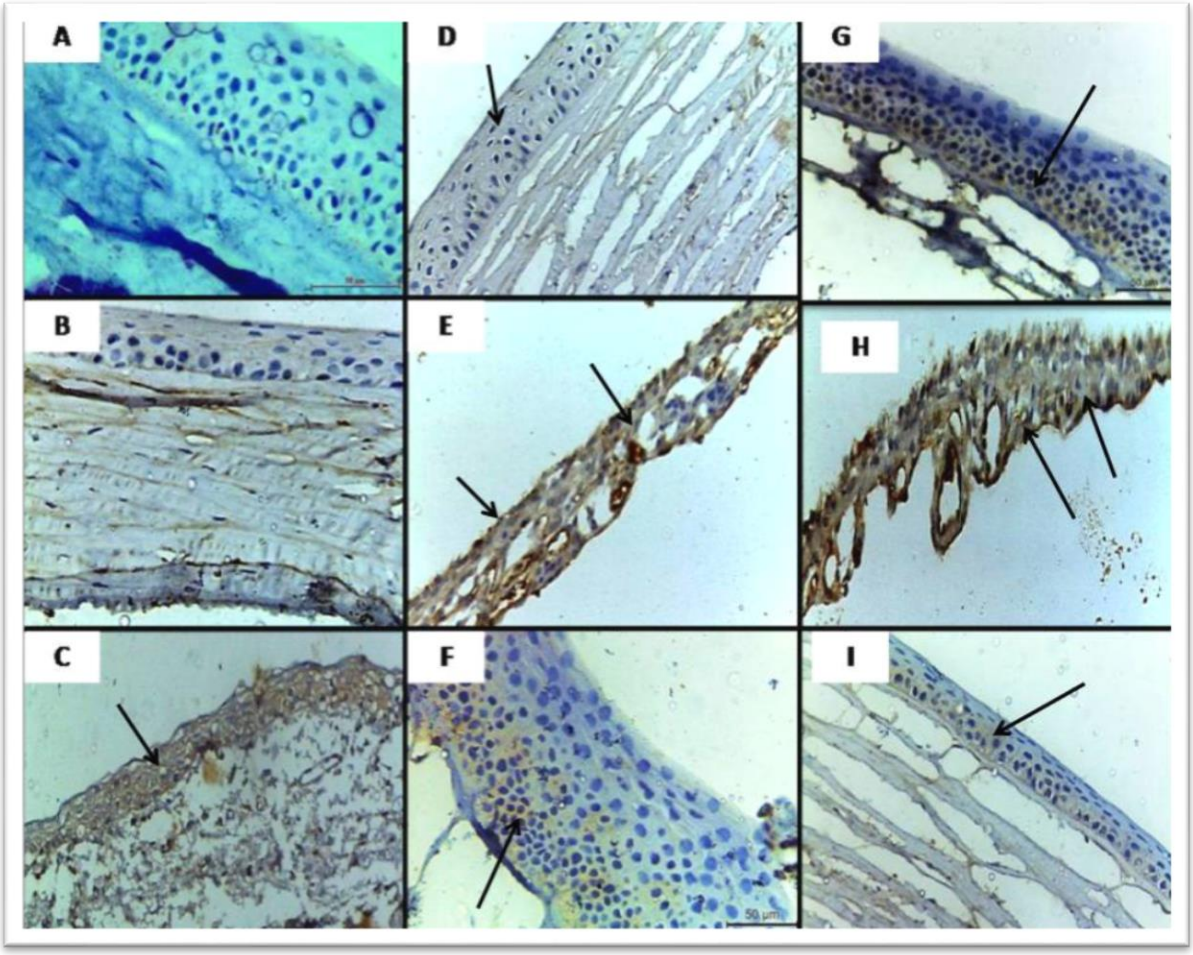

Fig. 9: Photomicrohraphs of TGF-β stained sections of the different study groups, A: normal control group, B: DK group day 0, C: diabetic ulcer group day 0, D: DK group day 2, E: diabetic ulcer group day 2, F: AgNps treated group day 2, G: DK group day 7, H: diabetic ulcer group day 7, I: AgNps treated group day 7, arrows: immunoreactive cells.

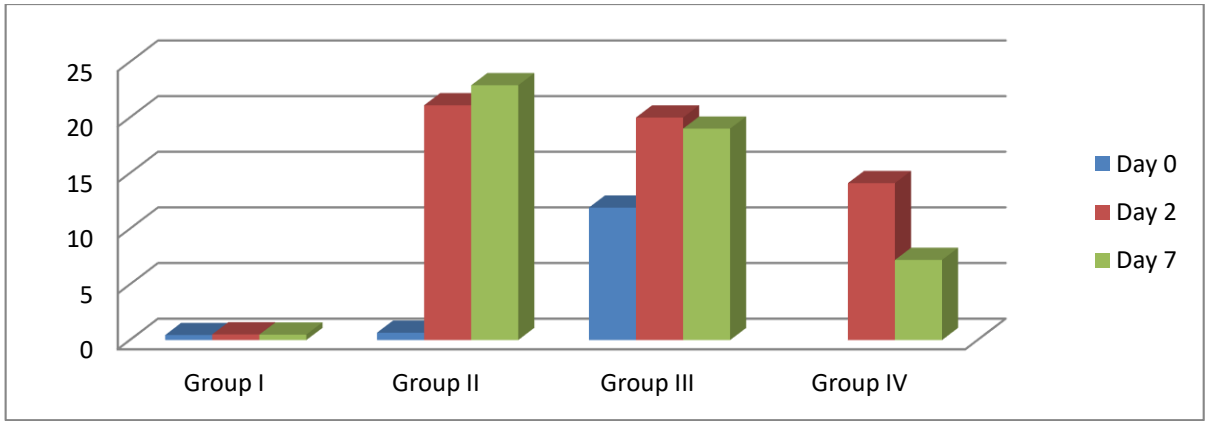

Fig. 10 : A histogram showing TGF-beta immunereactivity in different groups

Table 2: Mean values ±SD of MMP-9, Anti P75, IL-6, PDGF, ROS & MDA tissue levels among different groups (*n*=5)

Group	MMP-9 (pg/ml)	Anti P75 (pg/ml)	IL-6 (pg/ml)	PDGF (pg/ml)	ROS (nmol/ml)	MDA (nmol/ml)
Control						
Day 0	11.45±0.6	99.5±0.5	48.12±1	53.15±1.1	103±2	0.37±0.1
Day 2	11.42±0.3	100.72±0.7	49.95±0.9	52.74±0.8	105±2	0.39±0.1
Day 7	11.51±1.2	97.38±0.7	50.83±0.9	54.92±0.9	101±1	0.41±0.1
DK						
Day 0	11.82±1.3	103.12±1	59.12±1.4	53.11±1.4	106±1	0.42±0.1
Day 2	16.53±1.7*	78.24±1.7*	68.54±1.2*	67.94±1.9*	121±1*	0.59±0.1*
Day 7	20.61±1.1*	64.87±0.3*	74.32±1.8*	73.62±2*	137±2*	0.67±0.1*
Diabetic ulcer						
Day 0	14.29±0.6*	139.97±3.2*	98.74±2.1*	111.36±2*	129±1*	0.99±0.1*
Day 2	23.78±1.3*	137.34±2.9*	99.54±1.4*	108.65±1.9*	132±3*	0.99±0.1*
Day 7	30.18±1.7*	129.64±3*	89.12±1.7*	103.92±2.3*	153±3*	0.97±0.1*
Ag-Nps treated						
Day 2	22.32±1.4*	119.17±2.3*	61.14±1*	61.53±0.7*	113±2*	0.53±0.1*
Day 7	29.36±1*	118.28±2.1*	54.36±1.1*	59.94±0.8*	112±2*	0.51±0.1*

* : statistically significant when compared to control group ($p \leq 0.05$), SD: standard deviation.

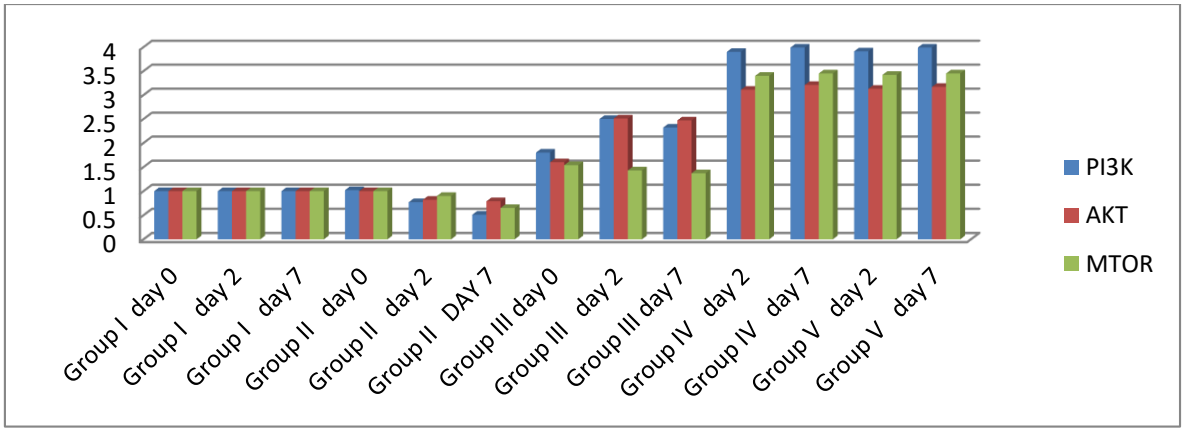

Fig. 11: A Histogram elaborating expression of PI3K, AKT, MTOR genes in the different study groups on the 3 time points of the study (day 0, 2 and 7).

DISCUSSION

In the present study, alloxan monohydrate drug was used to create a diabetic rat model. Alloxan is one of the well-known drugs used in animal studies for induction of Type I diabetes mellitus; several workers used alloxan monohydrate successfully to establish diabetic animal models ***(Solikhah et al., 2020*** and ***Sekiou et al., 2021).*** Alloxan is selectively toxic to beta cells of the pancreas; it accumulates as glucose analogues, and its cytotoxic effect is mediated by ROS ***(Lenzen et al., 2008)***.

In the present work, light microscopic examination of Hx&E stained sections from the DK group revealed variable cellular changes in the corneal epithelium; epithelial spongiosis, hyperchromatosis, pyknosis and karyolysis. Many authors reported similar epithelial alterations in diabetic keratopathy rats models ***(Alwafi et al., 2020*** and ***Nahar et al., 2021).*** The former author advocated the corneal epithelial changes in DM to the accumulation of advanced glycation end products (AGEs) and increased osmotic stress; AGEs affect normal cellular enzymatic activity and arrest cell growth and proliferation. ***Aseta et al. (2016)*** explained the cytoplasmic vacuolation as a form of programmed cell death (type III cytoplasmic cell death) that is triggered by insulin-like growth factor (IGF-1) and tumor necrosis factor (TNF) elevated in DM.

In the current work, pre-apoptic cellular findings were denoted in most corneal sections harvested on day seven of diabetic keratopathy group. Several previous studies elaborated that hyperglycemia directly affect the tissue levels of epithelial growth factor receptor (EGFR), nerve growth factor (NGF) and transforming growth factor beta (TGF β) with consequential reduction in the epithelial cellular proliferation ***(Bettahi et al., 2014*** and ***Shih et al., 2017).*** Corneal stroma of DK group showed disrupted normal architecture; in the form of disarrangement of the regular collagen lamellae and increased spacing in between them. The stroma also showed neovascularization and inflammatory cellular infiltration, ***Massoud et al. (2019)*** elaborated similar findings, they attributed the increased spacing of stromal lamellae to altered cellular properties in DM; electron transport chain changes, mitochondrial failure in addition to free radicals deposition, ***Hashem (2020)*** pointed out that vascular endothelial growth factor (VEGF) receptors play a crucial role in corneal avascularity through binding with the free VEGF making it unavailable for binding to receptors on cell membranes. ***Liu et al. (2022)*** assumed that neovascularization observed in DK is secondary to corneal inflammation and edema.

In the present work, corneal ulcer was induced in anesthetized rats using diluted solution of 1M NaOH. According to ***Zhang et al. (2022)*** the application of diluted NaOH causes severe inflammation and necrosis to the corneal epithelial cells and induces corneal ulceration. In the current work, light microscopic examination of Hx&E-stained sections of diabetic ulcer group cornea harvested on day zero, revealed remarkable epithelial affection; most sections showed complete denudation of the epithelium from the underlying stroma. The stromal collagenous lamellae were disrupted, mononuclear cellular infiltration and invasion with small blood vessels was elucidated in between the irregularly dispersed collagen fibers of the stroma. ***Portela et al. (2021)*** elaborated similar results in immediate corneal ulcer induced in animal models. Diabetic ulcer group cornea collected on the second day showed focal areas of epithelial discontinuity, superficial desquamation and stromal collagen disorganization with extensive neovascularization and inflammatory cellular infiltration. ***Hamil et al. (2013)*** classified the phases of corneal ulcer into four phases including immediate, acute, early repair and late repair phases. In the acute phase; 24 to 48 hours post induction of corneal ulcer, epithelial rejuvenation starts if there are enough amount of basal progenitor cells. In the current work, cornea of diabetic ulcer group harvested on day seven; showed evident cell apoptosis; hyperchromatic, pyknotic and karyolytic nuclei were elucidated in most sections. Stromal lamellae, Descemet's membrane and endothelial cell layer showed focal detachment or complete disruption, in addition to inflammatory cell infiltrates and extensive neovascularization.

In the current work, cornea of diabetic ulcer group collected on day two and seven showed extensive stromal neo-vascularization. ***Dan et al. (2008)*** exhibited corneal vascularization 48 hours post corneal alkali burn induction in rats, they advocated this to initiated tissue hypoxia and subsequently over proliferation of the capillary endothelial cells, along with increased expression of VEGF, EGF and TGF-β. In agreement with the present work, ***Yao et al. (2012)*** found that corneal alkali burns lead to exposure of basal epithelial layer due to necrosis and desquamation of the superficial and middle cellular layers, in addition, epithelial cells are overlapped into denuded zones, signifying attempts of re-epithelialization by epithelial migration from the healthy corneal epithelium to zones of epithelial defect.

In our work, group IV received daily subconjunctival injection of low concentration of silver nanoparticles (AgNps) for seven days. Used AgNps was 20 to 100 nm in size. ***Kim et al. (2021)*** used the same size of AgNps in animal model for corneal ulcer. Nanomaterials' chemical and physical properties depend on the size of the particles, which differ from conventional bulk materials. Silver owes its antibacterial and antifungal properties to its ionic form of silver only, which is unstable and can be easily inactivated by unwanted precipitation, with less healing properties ***(Kim et al., 2021)***. Light microscopic examination of corneal sections of AgNps-treated group elaborated restored normal histological architecture in most corneae. On the second day, many sections showed evident epithelial rejuvenation at multiple sites and decreased cellular apoptosis. Furthermore, corneae harvested on the seventh day showed epithelial regeneration, re-arranged stromal collagen fibers, intact Descemet`s membrane and endothelium. Multi-layered appearance of the corneal epithelium was restored in many sections. ***Alarcon et al. (2016)*** agreed with our finding; the authors have successfully shown that AgNps incorporated into collagen-based corneal implants can promote regeneration of corneal tissues and nerves, as an alternative to donor corneas for transplantation. In agreement with our work, ***Habibollah et al. (2014)*** have demonstrated that AgNPs was able to

promote epithelial regeneration and wound healing, through their powerful antibacterial properties, as well as their ability to decrease inflammation.

In the current study, morphometric measurement of corneal sections from DK group revealed a significant decrease in the total corneal thickness compared to control group. Similar results were elicited by ***Massoud et al. (2019)*** and ***Nahar et al. (2021).*** Previous studies assumed that the corneal thinning may be secondary to cellular hypoxia ***(Aseta et al., 2016).*** Others advocated the decrease in corneal thickness to cellular degeneration and slow rate of regeneration, due to accumulation of AGE ***(Elwan and Kassab, 2017).*** Statistical analysis of our work elaborated a significant decrease in the total corneal thickness in diabetic ulcer group sacrificed on day zero, compared to control group and DK group, sacrificed on the same days. In diabetic ulcer group, corneae collected on day two showed a significant increase in total corneal thickness, compared to day zero, and corneae collected on day seven also was significantly increased, compared to days zero and two. However, total corneal thickness in the diabetic ulcer group on day seven, was statistically indifferent from diabetic keratopathy group of the same day. Statistical analysis of the current work showed a significant increase in the total corneal thickness in AgNps treated group, obtained on days two and seven, when compared to corneae of DK and diabetic ulcer group obtained on the same days.

In the present work, PAS-stained sections of DK group revealed weak PAS reaction in addition to areas of endothelial basement membrane disruption, similar results were deduced by ***Fattah et al.(2021).*** Morphometric analysis of PAS-stained sections of our work revealed increased thickness of Descemet's membrane in corneae of diabetic keratopathy group versus control group. In agreement with this ***Karaca et al. (2022)*** elicited increased Descemet's membrane thickness in diabetic albino rat models. The latter workers explained that finding by the altered intracellular pH value of the corneal endothelium, resulting in decreased barrier effectiveness and failure of cellular pump function. In the present work, diabetic ulcer group elicited a significant decrease in Descemet's membrane thickness, compared to DK group and control group, in rats collected on days zero and two, ***Ibrahim et al. (2019)*** showed similar results in corneal ulcer animal models due to failure of proto-collagen deposition, cross linking of collagen fibrils and degeneration of endothelial cells. Histomorphometric analysis of PAS-stained sections revealed increased Descemet's membrane thickness in AgNps treated group. Its thickness was significantly increased, versus diabetic ulcer group on days two and seven. ***Kalishwaralal et al. (2010)*** observed the effect of nanosilver on ocular endothelial cells in DM; it showed normo-tonic cellular morphology. As endothelium is the major target for many therapies, it has been reported that AgNPs is an inhibitor of angiogenesis ***(Kalishwaralal et al., 2010).***

In DK group, morphometric analysis of MMP-2 stained sections elaborated increased mean area % of immunoreactivity; cornea harvested on days two and seven showed a significant increase when compared to control group corneae collected on the corresponding days. MMPs has a crucial role in stromal lamellae architecture and development of corneal neovascularization, specifically MMP-2 and MMP-9. ***Symeonides et al. (2013)*** detected elevated levels of MMP-2 and MMP-9 in tear samples of type I DM patients. Several animal studies elaborated increased MMP-2 level in diabetic rat models ***(Zhu et al., 2019*** and ***Li et al., 2020).*** Neovascularization is regulated by MMPs; it can degrade the basal membranes and extracellular matrix surrounding the sprouting capillaries and angiogenic growth factors, such as VEGF and TGF alpha and beta ***(Li et al., 2020).*** Increased expression of MMP-2 in the current

immunohistochemical work can explain the extensive neovascularzaton detected in most corneal sections of diabetic keratopathy group. Histomorphometric analysis of the current study elaborated increased mean area % of positive immunostaining of TrKA in DK group, in corneae harvested on day seven. TrKA, is expressed in the cornea during several pathological conditions that compasses re-innervation such as DM; it promotes epithelial colony formation and proliferation ***(Cellini et al., 2006).*** Moreover, clinical trials phase I have shown that recombinant human TrKA eye drops are well tolerated and safe in the treatment of resistant corneal ulcers ***(Sacchetti et al., 2020).*** In the current study, immunohistochemical work also elicited increased mean area % of positive reaction to TGF-β antibodies in DK corneae, harvested on days two and seven. ***Massoud et al. (2019)*** elaborated elevated tissue levels of TGF-β in diabetic rat model. ***Wilson et al. (2021)*** stated that the major mechanism for activation of TGF-β is through cell wall integrins; after extensive apoptosis in the corneal epithelium, TGF-β stimulate the transformation of stromal keratocytes into myofibroblasts to modulate healing.

In diabetic ulcer group, immunohistochemical study emphasized the pathological alterations; it elicited a significant increase in the mean area % of positive reaction of TrKA and TGF-β in corneae collected on days zero, two and seven, compared to control group and DK group, sacrificed on the same days. Differently, MMP-2 mean area % of immunostaining was elevated on days two and seven only. ***Yi and Zou (2019)*** reported increased gene expression of TGF-β1 and MMP-9 after corneal alkali burn. In accordance with our study***, Liu et al. (2022)*** elaborated increased expression of TrKA after corneal insult.

Biochemical analysis of corneal tissue extracted from DK group harvested on days two and seven, elaborated a significant increase in MMP-9 tissue enzyme, compared to control group cornea collected on the corresponding days; this goes hand in hand with the previous findings of our work regarding MMP-2 immune marker. ***Yar et al. (2012)*** reported similar findings. Diabetic environment stimulates the secretion of several MMPs that are assumed to have dual role in the development of diabetic keratopathy; in the early stages of the disease, MMP-9 facilitate cell apoptosis possibly through damaging the mitochondria, and in the later phase, it leads to neovascularization ***(Kowluru et al., 2017).*** DK group also elicited decreased tissue levels of anti p75 enzyme on days two and seven, that decrease was statistically significant compared to control group cornea collected on the corresponding days. A strong link between anti P75 and diabetic oculopathy has become apparent after two prospective clinical trials, the Fenofibrate Intervention and Event Lowering in Diabetes (FIELD study) and the Action to Control Cardiovascular Risk in Diabetes (ACCORD) study, that both reported that fenofibrate, an anti P75 was effective in improving diabetic retinopathy in type 2 diabetes ***(Matlock et al., 2020).*** Diabetic keratopathy cornea extracted on the 2nd and 7th day, both showed elevated tissue levels of IL-6 and PDGF, they both elaborated a significant increase when compared to control cornea extracted on the same days. In agreement with our results, ***Ghasemi et al. (2018)*** reported elevated interleukins and PDGF in DK. Anti-IL-6 targeted immunotherapy has recently been employed as an important treatment modality in IL-6 related ocular disorders (***Ghasemi et al., 2018).*** In the current study, diabetic ulcer group also elicited elevated tissue levels of anti p75 and MMP 9 on days two and seven, they both showed a statistically significant increase compared to control and diabetic keratopathy groups, sacrificed on the corresponding days. Interestingly, PDGF and IL-6 started to show a significant elevation since day zero

of corneal ulcer induction. A series of studies emphasized the important role of PDGF and ILs in the repair process. Upon injury, PDGF is released instantly from degranulated platelets and presented in the ulcer inflammatory fluid, stimulating a pathological cascade of ILs production and release, particularly early after injury ***(Zhang et al., 2022).*** In addition to that, AgNps treated rats elicited lower tissue levels of MMP 9 and anti P75 on days two and seven, this decrease was statistically significant when compared to DK and diabetic ulcer ulcer groups harvested on the corresponding days. On another hand, in AgNps treated group, PDGF and IL6 tissue levels decreased significantly, in comparison to diabetic ulcer group, the latter treatment was superior to AgNps in improving tissue levels of PDGF and IL-6. ***Li et al. (2020)*** pointed out that PDGF, IL-6 and other several inflammatory mediators were decreased with the use of silver nanoparticle-loaded collagen-chitosan dressing .

In our study, diabetic keratopathy group showed statistically significant rise of MDA and ROS tissue levels, versus control group. ***Rapala et al. (2021)*** have reported elevated oxidative stress markers; ROS and MDA, in diabetic rats' cornea. As for AgNps treated group, it exhibited increased tissue levels of ROS and MDA, the increase was statistically insignificant when compared to DK group, ***Chairuangkitti et al. (2013)*** disagreed with our work; they assumed that AgNps contribute to cell death by triggering ROS generation. This may be true in tumor cells only, as silver nanoparticles are used in higher concentrations.

In the present study, PI3K, AKT and MTOR genes were significantly down regulated in DK group cornea of day seven, compared to control group sacrificed on the same day. Previous authors agreed with our work ***(Peterson et al., 2022).*** The latter assumed that diabetes-associated hyperglycemia directly inhibit PI3K/AKT signaling by increasing ROS and endoplasmic reticulum (ER) stress levels. Others advocated the decreased expression of PI3K/AKT/MTOR genes to the suppression of growth factors receptors in hyperglycemic state of DM ***(Liu et al., 2022).*** The current study elicited a significant increase in the expression of PI3K, AKT and MTOR genes in the diabetic ulcer group (days zero, two, and seven) versus DK and control groups. Previous workers reported upregulation of PI3K/AKT/MTOR axis in corneal ulcer disease ***(Peterson et al., 2022).*** Real time PCR of AgNps treated cornea showed activated PI3K/AKT/MTOR pathway on days two and seven of the experiment, the upregulated values were statistically significant when compared to DK and ulcer groups rats, ***Chang et al. (2021)*** elucidated similar findings.

Conclusion

We concluded from the current work that silver nanoparticles (AgNps) can be a promising alternative to conventional bulky silver containing formulas in corneal ulcer treatment; it can promote epithelial wound healing, matrix reconstruction and upregulate cellular proliferation signaling pathway.

We recommend regular follow up in diabetic patients, in order to avoid its adverse effects on the cornea. In cases of resistant corneal ulcers in DM, silver nanoparticles chelated vehicles can successfully accelerate epithelial wound healing and support corneal integrity.

References

1. Afifi, M., & Abdelazim, A. M. (2015). Ameliorative effect of zinc oxide and silver nanoparticles on antioxidant system in the brain of diabetic rats. *Asian Pacific Journal of Tropical Biomedicine*, *5*(10), 874-877.

2. Alarcon, E. I., Vulesevic, B., Argawal, A., Ross, A., Bejjani, P., Podrebarac, J. & Griffith, M. (2016). Coloured cornea replacements with anti-infective properties: expanding the safe use of silver nanoparticles in regenerative medicine. *Nanoscale*, *8*(12), 6484-6489.

3. Alwafi, H. A., algahdali, E. H., Aljehany, B. M., Altamimi, S. R., Alwafi, H., & Alfayez, A. (2020). Soad Shaker, Hailah Mohammed Almohaimeed. Virgin Olive Oil Protects the Cornea against Diabetes-Induced Damage in Rats: A Biochemical and Histological Study. *Medical Science*, *24*(105), 3438-3446.

4. Aseta, F. B., Mwachaka, P. M., Odula, P. O., & Malek, A. K. (2016). Histomorphological changes in the cornea of the rat following monocular eyelid closure. *Anatomy*, *10* (2), 87-93.

5. Bettahi, I., Sun, H., Gao, N., Wang, F., Mi, X., Chen & Yu, F. S. X. (2014). Genome-wide transcriptional analysis of differentially expressed genes in diabetic, healing corneal epithelial cells: hyperglycemia-suppressed tgfβ3 expression contributes to the delay of epithelial wound healing in diabetic corneas. *Diabetes*, *63* (2), 715-727.

6. Butler, K. S., Peeler, D. J., Casey, B. J., Dair, B. J., & Elespuru, R. K. (2015). Silver nanoparticles: correlating nanoparticle size and cellular uptake with genotoxicity. *Mutagenesis*, *30*(4), 577-591.

7. Cellini, M., Bendo, E., Bravetti, G. O., & Campos, E. C. (2006). The use of nerve growth factor in surgical wound healing of the cornea. *Ophthalmic research*, *38*(4), 177-181.

8. Chairuangkitti, P., Lawanprasert, S., Roytrakul, S., Aueviriyavit, S., Phummiratch, D., Kulthong, K. & Maniratanachote, R. (2013). Silver nanoparticles induce toxicity in A549 cells via ROS-dependent and ROS-independent pathways. *Toxicology in vitro*, *27*(1), 330-338.

9. Chang, Y. S., Tai, M. C., Ho, C. H., Chu, C. C., Wang, J. J., Tseng, S. H., & Jan, R. L. (2020). Risk of corneal ulcer in patients with diabetes mellitus: a retrospective large-scale cohort study. *Scientific Reports*, *10*(1), 7388.

10. Dan, L., Shi-long, Y., Miao-li, L., Yong-ping, L., Hong-jie, M., Ying, Z., & Xiang-gui, W. (2008). Inhibitory effect of oral doxycycline on neovascularization in a rat corneal alkali burn model of angiogenesis. *Current eye research*, *33*(8), 653-660.

11. Elwan, W. M., & Kassab, A. A. (2017). The potential protective role of hesperidin against capecitabine-induced corneal toxicity in adult male albino Rat. Light and electron microscopic study. *Egyptian Journal of Histology*, *40*(2), 201-215.

12. Fattah, I. O. A., Madani, G. A., & El-Din, W. A. N. (2021). Topical onion juice mitigates the morphological alterations of the cornea in the aged male rats. *Anatomy & Cell Biology*, *54*(3), 375-386.

13. Ghasemi, H. (2018). Roles of IL-6 in ocular inflammation: a review. *Ocular immunology and inflammation*, *26*(1), 37-50.

14. Habiboallah, G., Mahdi, Z., Majid, Z., Nasroallah, S., Taghavi, A. M., Forouzanfar, A., & Arjmand, N. (2014). Enhancement of gingival wound healing by local application of silver nanoparticles periodontal dressing following surgery: a histological assessment in animal model. *Modern Research in Inflammation*, *2014*.

15. Hamill, C. E., Bozorg, S., Chang, H. Y. P., Lee, H., Sayegh, R. R., Shukla, A. N., & Chodosh, J. (2013). Corneal alkali burns: a review of the literature and proposed protocol for evaluation and treatment. *International ophthalmology clinics*, *53*(4), 185-194.

16. Hashem, H. R. (2020). Regenerative and Antioxidant Properties of Autologous Platelet-Rich Plasma Can Reserve the Aging Process of the Cornea in the Rat Model. *Oxidative Medicine and Cellular Longevity*, *2020*.

17. Ibrahim, M., & Elswaidy, N. (2019). A histological and immunohistochemical study of the effect of platelet-rich plasma

on a corneal alkali burn in adult male albino rat. *Egyptian Journal of Histology*, *42*(2), 482-495.

18. Kalantari, K., Mostafavi, E., Afifi, A. M., Izadiyan, Z., Jahangirian, H., Rafiee-Moghaddam, R., & Webster, T. J. (2020). Wound dressings functionalized with silver nanoparticles: promises and pitfalls. *Nanoscale*, *12*(4), 2268-2291.

19. Kalishwaralal, K., barathmanikanth, S., Pandian, S. R. K., Deepak, V., & Gurunathan, S. (2010). Silver nano—a trove for retinal therapies. *Journal of Controlled Release*, *145*(2), 76-90.

20. Karaca, Ç., Akdoğan, M., Demirel, H. H., & Ünal, C. (2022). The Effects of Systemic Coenzyme Q10 Treatment on Corneal Histology in Streptozocin-Induced Diabetic Rats. *Ocular Immunology and Inflammation*, 1-7.

21. Kim, S., Gates, B. L., Chang, M., Pinkerton, K. E., Van Winkle, L., Murphy, C. J. & Thomasy, S. M. (2021). Transcorneal delivery of topically applied silver nanoparticles does not delay epithelial wound healing. *Nanoimpact*, *24*, 100352.

22. Kowluru, R. A., & Shan, Y. (2017). Role of oxidative stress in epigenetic modification of MMP-9 promoter in the development of diabetic retinopathy. *Graefe's Archive for Clinical and Experimental Ophthalmology*, *255*, 955-962.

23. Kramerov, A. A., Shah, R., Ding, H., Holler, E., Turjman, S., Rabinowitz, Y. S., ... & Ljubimov, A. V. (2021). Novel nanopolymer RNA therapeutics normalize human diabetic corneal wound healing and epithelial stem cells. *Nanomedicine: Nanotechnology, Biology and Medicine*, *32*, 102332.

24. Lenzen, S. (2008). The mechanisms of alloxan-and streptozotocin-induced diabetes. *Diabetologia*, *51*(2), 216-226.

25. Li, W., Wang, X., Cheng, J., Li, J., Wang, Q., Zhou, Q. & Xie, L. (2020). Leucine-rich α-2-glycoprotein-1 promotes diabetic corneal epithelial wound healing and nerve regeneration via regulation of matrix metalloproteinases. *Experimental Eye Research*, *196*, 108060.

26. Liu, G., Chen, L., Cai, Q., Wu, H., Chen, Z., Zhang, X., & Lu, P. (2018). Streptozotocin-induced diabetic mice exhibit reduced experimental choroidal neovascularization but not corneal neovascularization. *Molecular medicine reports*, *18*(5), 4388-4398.

27. Majeed, W., Khaliq, T., Aslam, B., & Khan, J. A. (2018). Polyherbal Formulation Prevents Hyperglycemia by Modulating the Biochemical Parameters and Upregulating the Insulin Signaling Cascade in Alloxan Induced Hyperglycemic Rats. *Pakistan Veterinary Journal*, *38*(2).

28. Massoud, A. M. A., El Ebiary, F. H., Al-khalek, H. A. A., & Gawad, S. A. (2019). Possibl e therapeutic role of fermented deglycyrrhizinized liquorice extract o n experimentally induced diabetic keratopathy in Rats. *Histological Study. Cyto l Histol Rep*, *2*, 107.

29. Matlock, H. G., Qiu, F., Malechka, V., Zhou, K., Cheng, R., Benyajati, S., ... & Ma, J. X. (2020). Pathogenic role of pparα Downregulation in corneal nerve degeneration and impaired corneal sensitivity in diabetes. *Diabetes*, *69*(6), 1279-1291.

30. Mauricio, M. D., Guerra-Ojeda, S., Marchio, P., Valles, S. L., Aldasoro, M., Escribano-Lopez, I. & Victor, V. M. (2018). Nanoparticles in medicine: a focus on vascular oxidative stress. *Oxidative Medicine and Cellular Longevity*, *2018*.

31. Mihai, M. M., Dima, M. B., Dima, B., & Holban, A. M. (2019). Nanomaterials for wound healing and infection control. *Materials*, *12*(13), 2176.

32. Nahar, N., Mohamed, S., Mustapha, N. M., Lau, S., Ishak, N. I. M., & Umran, N. S. (2021). Metformin attenuated histopathological ocular deteriorations in a streptozotocin-induced hyperglycemic rat model. *Naunyn-Schmiedeberg's Archives of Pharmacology*, *394*, 457-467.

33. Peterson, C., & Chandler, H. L. (2022). Insulin facilitates corneal wound healing in the diabetic environment through the RTK-

PI3K/Akt/mtor axis in vitro. *Molecular and cellular endocrinology*, *548*, 111611.

34. Portela, A. L. B. M., Moreno, R. N., Ribeiro, M. H. M. L., de Andrade, F. M., Alves, Y. V., Alves, M., & Lira, R. P. C. (2021). Role of nicergoline in corneal wound healing in diabetic rats. *BMC ophthalmology*, *21*(1), 1-6.

35. Priyadarsini, S., Whelchel, A., Nicholas, S., Sharif, R., Riaz, K., & Karamichos, D. (2020). Diabetic keratopathy: Insights and challenges. *Survey of ophthalmology*, *65*(5), 513-529.

36. Rąpała, K., Borymska, W., & Kaczmarczyk-Sedlak, I. (2021). Effectiveness of Magnolol, a Lignan from Magnolia Bark, in Diabetes, Its Complications and Comorbidities—A Review. *International Journal of Molecular Sciences*, *22*(18), 10050.

37. Rezvanian, M., Ng, S. F., Alavi, T., & Ahmad, W. (2021). In-vivo evaluation of Alginate-Pectin hydrogel film loaded with Simvastatin for diabetic wound healing in Streptozotocin-induced diabetic rats. *International Journal of Biological Macromolecules*, *171*, 308-319.

38. Sacchetti, M., Lambiase, A., Schmidl, D., Schmetterer, L., Ferrari, M., Mantelli, F., ... & Garhoefer, G. (2020). Effect of recombinant human nerve growth factor eye drops in patients with dry eye: a phase iia, open label, multiple-dose study. *British Journal of Ophthalmology*, *104*(1), 127-135.

39. Sekiou, O., Boumendjel, M., Taibi, F., Tichati, L., Boumendjel, A., & Messarah, M. (2021). Nephroprotective effect of Artemisia herba alba aqueous extract in alloxan-induced diabetic rats. *Journal of traditional and complementary medicine*, *11*(1), 53-61.

40. Shih, K., Lam, K. S., & Tong, L. (2017). A systematic review on the impact of diabetes mellitus on the ocular surface. *Nutrition & diabetes*, *7*(3), e251-e251.

41. Solikhah, T. I., Setiawan, B., & Ismukada, D. R. (2020). Antidiabetic activity of papaya leaf extract (Carica Papaya L.) Isolated with maceration method in alloxan-induced diabeticmice. *Systematic Reviews in Pharmacy*, *11*(9), 774-778.

42. Torabian, F., Akhavan Rezayat, A., Ghasemi Nour, M., Ghorbanzadeh, A., Najafi, S., Sahebkar, A. & Darroudi, M. (2022). Administration of silver nanoparticles in diabetes mellitus: a systematic review and meta-analysis on animal studies. *Biological Trace Element Research*, *200*(4), 1699-1709.

43. Wang, B., Yang, S., Zhai, H. L., Zhang, Y. Y., Cui, C. X., Wang, J. Y., & Xie, L. X. (2018). A comparative study of risk factors for corneal infection in diabetic and non-diabetic patients. *International journal of ophthalmology*, *11*(1), 43.

44. Wilson, S. E. (2021). Interleukin-1 and transforming growth factor beta: Commonly opposing, but sometimes supporting, master regulators of the corneal wound healing response to injury. *Investigative ophthalmology & visual science*, *62*(4), 8-8.

45. Yao, L., Li, Z. R., Su, W. R., Li, Y. P., Lin, M. L., Zhang, W. X., ... & Liang, D. (2012). Role of mesenchymal stem cells on cornea wound healing induced by acute alkali burn. *Plos one*, *7*(2), e30842.

46. Yar, A. S., Menevse, S., Dogan, I., Alp, E., Ergin, V., Cumaoglu, A., ... & Menevse, A. (2012). Investigation of ocular neovascularization–related genes and oxidative stress in diabetic rat eye tissues after resveratrol treatment. *Journal of Medicinal Food*, *15*(4), 391-398.

47. Yeung, V., Sriram, S., Tran, J. A., Guo, X., Hutcheon, A. E., Zieske, J. D., & Ciolino, J. B. (2021). FAK inhibition attenuates corneal fibroblast differentiation in vitro. *Biomolecules*, *11*(11), 1682.

48. Yi, Q., & Zou, W. J. (2019). The wound healing effect of doxycycline after corneal alkali burn in rats. *Journal of Ophthalmology*, *2019*.

49. Zhang, L., Yu, J. C., Yip, H. Y., Li, Q., Kwong, K. W., Xu, A. W., & Wong, P. K. (2003). Ambient light reduction strategy to synthesize silver nanoparticles and silver-coated tio2 with enhanced photocatalytic

and bactericidal activities. *Langmuir*, *19*(24), 10372-10380.

50. Zhang, S., Li, P., Yuan, Z., & Tan, J. (2019). Platelet-rich plasma improves therapeutic effects of menstrual blood-derived stromal cells in rat model of intrauterine adhesion. *Stem cell research & therapy*, *10*, 1-12.

51. Zhu, L., Titone, R., & Robertson, D. M. (2019). The impact of hyperglycemia on the corneal epithelium: molecular mechanisms and insight. *The Ocular Surface*, *17*(4), 644-654.